Pergamon

Solid State Communications, Vol. 107, No. 4, pp. 171–176, 1998

0038–1098/98 $19.00+.00

PII: S0038-1098(98)00170-7

DETERMINATION OF Ni^{2+} CONCENTRATION DEPENDENCE OF THE NONLINEAR REFRACTIVE INDEX OF $BaLiF_3 : Ni^{2+}$ CRYSTAL BY THE RESONANT Z-SCAN METHOD

R.E. Samad,*,† S.L. Baldochi, S.P. Morato and N.D. Vieira Jr

Instituto de Pesquisas Energéticas e Nucleares, CP 11049, CEP 05422-970, São Paulo, SP, Brazil

(*Received* 25 *November* 1997; *accepted* 30 *March* 1998 *by R.T. Phillips*)

The resonant Z-Scan technique was used to measure the real and imaginary parts of the nonlinear refractive index of a new material, the Ni^{2+} doped $BaLiF_3$ crystal. We used four different dopant concentrations and could determine the concentration dependence behavior of the nonlinear macroscopic parameters. The microscopic (local) nonlinear parameters per ion were determined and for low Ni^{2+} concentrations they are constant. The excited state absorption cross section was estimated in first-order and it has the same magnitude of the ground state absorption cross section.

Keywords: C. point defects, D. optical properties, E. nonlinear optics, E. light absorption and reflection.

1. INTRODUCTION

The $BaLiF_3 : Ni^{2+}$ crystal [1] is a potentially laser active medium due to its great similarity to the $KMgF_3$ host crystal, that has already shown laser action when doped with divalent transition metals (Co^{2+} and Ni^{2+}) [2, 3]. As an advantage, it can be pumped by a Nd : YAG laser and presents a broad emission band centered at 1.5 μm [4]. In usual laser operation conditions, the crystal is under influence of strong electromagnetic fields, providing the occurrence of nonlinear effects [5, 6]. Among these effects is the self-focusing [7, 8] (or self-defocusing) of a gaussian beam, where the high intensities of the electric field modify the refractive index of the medium [9]. This refractive index change turns the sample into a lenslike medium, modifying the resonant optical properties of the cavity [10]. To take these physical changes into account in the designing of the cavity, we must know the value of the nonlinear refractive index of the laser medium.

In order to determine the real and imaginary parts of the nonlinear refractive index of the Ni^{2+} doped $BaLiF_3$ crystal, we used the Z-Scan technique [11]. This single beam technique, introduced in 1989 [12], transforms a phase modulation in an amplitude modulation of the laser beam. The analysis of the amplitude modulation gives the nonlinear refractive index. Since its introduction, the technique has suffered many modifications to improve its sensitivity [13, 14], to measure the nonlinear coefficients of highly absorptive or opaque samples [15, 16] and to study the mechanisms that originate the nonlinearity [17–19], among others.

2. THEORY

We utilized a modification of the Z-Scan technique, introduced by Oliveira *et al.* [20], where the sample under study is a saturable absorber and therefore the associated nonlinearity is due to a slow population change. In this case, the total variation of the nonlinear refractive index of the medium is described by [21]

$$\delta n = \frac{2\pi N_0}{9}\frac{(n_0^2+2)^2}{n_0}(\alpha_3-\alpha_1)\frac{I/I_S}{1+I/I_S}(1-e^{-t/\tau_{ef}}), \tag{1}$$

where N_0 is the dopant density, n_0 the refractive index of the medium, I the laser intensity, I_S the saturation intensity of the sample. The local field correction term was taken explicitly into consideration [22]. The effective lifetime of the resonant transition is given by $\tau_{ef}^{-1} = \tau^{-1} + \sigma_1 I$, where τ is the lifetime of the excited state and σ_1 the absorption cross-section of the transition involved. The linear polarizabilities α_3 and α_1 of the

* Corresponding author.
† E-mail: resamad@net.ipen.br

excited and ground states, respectively, represent the amount of deformation that the wavefunctions of the levels suffer when under the influence of an external electric field. In this formalism, after defining the third-order nonlinear effective hiperpolarizability by $\gamma_{eff} = (\alpha_3 - \alpha_1)$, the real ($n_2$) and imaginary ($\kappa_2$) parts of the nonlinear refractive index are given by

$$n_2 = \frac{2\pi N_0}{9}\left[\frac{n_0^2+2}{3}\right]^2 \frac{\gamma_{eff}}{I_S} \tag{2a}$$

$$\kappa_2 = 2\pi N_0 \frac{c}{\omega}\frac{\sigma_3 - \sigma_1}{I_S} \tag{2b}$$

where c is the speed of light, ω the frequency of the exciting light and σ_3 and σ_1 the excited and ground state absorption cross sections, respectively. The imaginary part of the nonlinear refractive index is named the nonlinear extinction coefficient of the sample.

When a two-photon (excited state) absorption process exists, the intensity of light attenuation is given by

$$\frac{dI}{dz'} = -\alpha I - \beta I^2, \tag{3}$$

where α is the linear absorption coefficient of the sample and β is the sample two-photon absorption coefficient; z' is the position inside the sample. Otherwise, the intensity of light attenuation in a saturable absorber is given by:

$$\frac{dI}{dz'} = -\frac{\alpha I}{1 + I/I_S} \cong -\alpha I + \frac{\alpha}{I_S} I^2 + O(3) \tag{4}$$

By considering the first-order expansion of the expression (4), we find that the effective nonlinear absorption coefficient (β_{eff}) of the sample is then given by the combination of (3) and (4):

$$\beta_{eff} = \beta - \frac{\alpha}{I_S}, \tag{5}$$

taking into account both the processes of nonlinear absorption and saturation. If $\beta_{eff} > 0$, excited state absorption processes dominate; if $\beta_{eff} < 0$, saturation processes dominate. The relation between the nonlinear absorption coefficient of the sample and its nonlinear extinction coefficient is given by

$$\beta_{eff} = 2\frac{\omega}{c}\kappa_2. \tag{6}$$

As we can see from (1), when a temporally modulated beam, with a Heaviside like behavior, excites a saturable absorber, the profile of refractive index variation, δn, evolves exponentially in time. In a Z-Scan experimental setup where the light intensity is modulated by a chopper, it means that the light intensity transmitted by the aperture in the far-field is expected to evolve exponentially in time, as can be seen in Fig. 1.

The technique [20] consists in modulating the laser beam by means of a chopper and measuring the beam intensity during the temporal evolution described by Fig. 1, in the times t_1 and t_2. In t_1 the sample transmittance is purely linear and in t_2 the linear and the nonlinear effects compose it. If we divide the signal in t_2 by the signal in t_1 we obtain the normalized nonlinear transmittance of the sample. Repeating this procedure for different positions along the beam path (and therefore different intensities), we obtain the Z-Scan curve. The resulting curve contains both the nonlinear phase and nonlinear absorption effects. In order to obtain the nonlinear phase information, the usual technique [11] of measuring the transmittance without the aperture is performed, providing only the nonlinear absorption effect. The ratio between the two curves provides the Z-Scan trace due only to the nonlinear phase.

The main advantage on the present method is that the changes in beam intensity are due only to the nonlinear effect, simplifying the experimental setup and the normalization. As a consequence of the saturation of the absorption, the variation of transmittance between peak and valley of the Z-Scan curve departs from the expression proposed by Sheik-Bahae [11]. Oliveira showed that this variation can be described by:

$$\Delta T_{pv} = 0.406(1-A)^{0.25(1+I_0/I_S)^{(1-A)}} \frac{|\Delta\Phi_0|}{(1 + I_0/I_S)^{0.525}}. \tag{7}$$

For the absorptive curve Oliveira showed that the peak transmittance is now described by:

$$T_p - 1 = k\kappa_2 L_{eff} \frac{I_0}{(1 + I_0/I_S)^{0.76}}. \tag{8}$$

In expression (7) the on-axis nonsaturated nonlinear phase is given by $\Delta\Phi_0 = kn_2 L_{eff} I_0$, where $k = 2\pi/\lambda$ is the wavenumber of the laser light (with λ being the laser

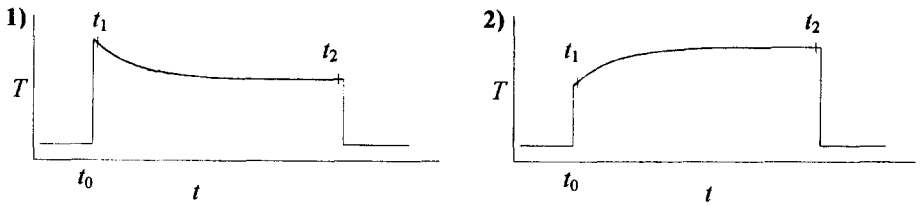

Fig. 1. Expected temporal evolution of the Z-scan transmittance for a positive (negative) nonlinear sample. In t_0 the chopper opens, transmitting the light. Curves 1 and 2 represent the signal when the sample is before (after) and after (before) the beamwaist, respectively.

wavelength), I_0 is the beam intensity at the beamwaist and $L_{eff} = (1 - e^{-\alpha L})/\alpha$ is the sample effective length. A is the iris aperture as defined by Sheik-Bahae.

3. EXPERIMENTAL SETUP

In this work we studied the Ni^{2+} doped $BaLiF_3$ crystal. An scheme of the conventional cell of the $BaLiF_3$ crystal is shown in Fig. 2. The crystal mix is cubic, with an inverted perovskite structure [23], where the monovalent and divalent cations invert their positions. The Ba^{2+} and Li^+ occupy the sites (0, 0, 0) and ($\frac{1}{2}$ $\frac{1}{2}$ $\frac{1}{2}$), respectively and three F^- complete the cell. When incorporated in the lattice, the Ni^{2+} substitutes the Li^+ [24, 25]. In Table 1 we present the physical parameters of the $BaLiF_3$ crystal.

We used a Nd : YAG laser oscillating in 1064 nm, to pump the $BaLiF_3 : Ni^{2+}$ crystal in its fundamental, broad, absorption band, centered at 1180 nm.

We have studied four different Ni^{2+} concentrations in the $BaLiF_3$ crystal. The samples were zone refined and then grown by the Czochralski technique in our facilities and their dopant concentrations were determined by X-ray fluorescence and Neutron activation techniques. In Table 2 the characteristics of the samples used are shown.

The experimental setup utilized is shown in Fig. 3. We used a modified CW TEM_{00} Quantronix Nd : YAG laser [26], oscillating in the 1064 nm line, to excite the samples in resonance with the fundamental absorption ($^3T_{2g} \rightarrow {}^3A_{2g}$) of the Ni^{2+} [4]. A 50 μm pinhole was used to spatially filter the beam and a chopper to modulate it. The sample was mounted in a micrometric translation stage controlled by computer, with minimal steps of 10 μm. We utilized Germanium detectors, one with and the other without an iris in its front. A lens was utilized to focalize the beam in the pinhole and the second and third lenses to configure the beam for the Z-Scan path. The lenses in front of the detectors were needed to compensate for their small detection areas. The signals were read in a TDS 684B Tektronix digital oscilloscope and transmitted to a computer, where they were analyzed.

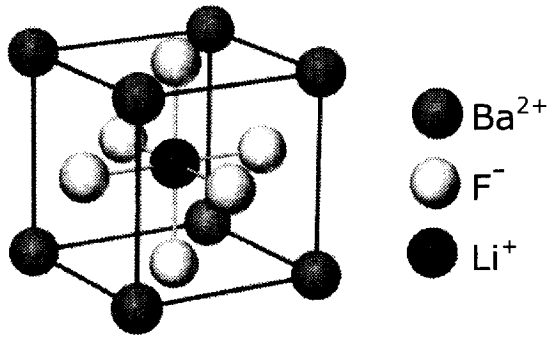

Fig. 2. Conventional cell of the $BaLiF_3$ crystal.

Table 1. Physical Parameters of the $BaLiF_3$ Crystal

Parameter	Value
Atomic Weight	201.263 g
Density	5.243 g/cm^3
Lattice Constant	3.995 Å
Refractive Index ($\lambda = 589$ nm)	1.544
Molecular Density	1.568×10^{22} ions/cm^3

4. EXPERIMENTAL RESULTS

In Fig. 4 is shown the experimental Z-Scan curve for the crystal with the smallest Ni^{2+} concentration (0.15 mol.%). First, the curve shows the typical trace for a negative nonlinear coefficient. The signal to noise ratio shown is still good (resolution $> \lambda/5000$). For the other higher dopant concentration samples, the curve profile is similar and the signal to noise ratio is even better.

In Fig. 5 it is presented a curve obtained without aperture for the sample with the highest Ni^{2+} concentration (1.9 mol.%). In this curve we can see an absorption saturation phenomenon, indicating that the nonlinear absorption coefficient of the sample is also negative.

The transmittance variation between peak and valley and the peak transmittance were normalized accordingly to expressions (7) and (8), respectively. We made several Z-Scan measurements for each sample and from their normalization we obtained the real and imaginary parts

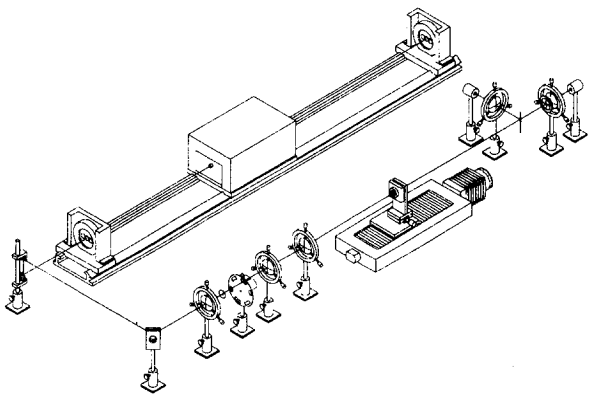

Fig. 3. Experimental setup scheme. A Nd : YAG laser (1064 nm) was used to excite the sample by presenting a focus along the sample path. The sample was moved along the path by a micrometric translator controlled by a computer. The signals were detected by two germanium detectors and analyzed in a digital TDS 684B Tektronix oscilloscope and then stored in a computer.

Table 2. Spectroscopic parameters of the utilized samples

Sample	Length (nm)	Ni^{2+} concentration mol.%	10^{19} cm^{-3}	Lifetime ms	σ 10^{-21} cm^2	I_S kW/cm^2	α cm^{-1}
0.15%	1.05(5)	0.15(2)	2.4(2)	2.8(3)	3.17(26)	21.0(27)	0.076(6)
0.30%	1.10(5)	0.33(4)	5.2(6)	2.8(3)	3.17(26)	21.0(27)	0.17(1)
1%	1.10(5)	0.9(1)	14(2)	2.8(3)	3.17(26)	21.0(27)	0.44(4)
2%	1.15(5)	1.9(2)	30(3)	2.0(3)	3.17(26)	29.9(56)	0.96(8)

of the nonlinear refractive index for each one of the Ni^{2+} concentrations.

Figure 6 shows the Ni^{2+} concentration dependence of the nonlinear coefficients. It is clearly seen that this dependence is linear up to 1 mol.% (14×10^{19} cm^{-3}) for the macroscopic parameters (n_2 and κ_2). For greater dopant concentrations the macroscopic parameters behavior deviate from the linear one. These results agree with the ones obtained by conventional spectroscopy [1] that shows that the lifetime of the first excited state is independent of the dopant concentration only for small concentrations.

From the macroscopic parameters results, we could calculate the microscopic parameters (γ_{eff} and β_{eff}/ion) for each sample. The calculated values for γ_{eff} and β_{eff}/ion are shown in the fourth and sixth columns of Table 3, respectively. These parameters represent the response of each individual dopant ion to the local electric field. Considering that the hiperpolarizability and the absorption cross-section are intrinsic ion parameters, we expect them to be independent of the dopant concentration in the sample. For the two samples with smallest concentration we observe that this occurs, confirming the negligible cooperative effects. The other two samples deviate from this constant, with the deviation increasing with the dopant concentration. These deviations towards greater values may be explained by the proximity of the Ni^{2+} ions. When the dopant concentration increases, the outer electron of a single Ni^{2+} ion starts to interact with the wavefunction of the neighbor Ni^{2+} ions and the Pauli exclusion principle must be taken into account. This confinates the electron, creating a greater (effective) restoration force, that in the anharmonic oscillator approximation requires a greater anharmonic [27] constant. This greater anharmonic constant generate a greater nonlinearity.

The negative values obtained for n_2 imply that $\gamma_{eff} = (\alpha_3 - \alpha_1)$ is negative and therefore $\alpha_1 > \alpha_3$ (α_1 and α_3 are positive, since they follow from the Clausius–Mossotti Relation [23]). This means that the ground state wavefunction is more deformed by the electric field then the excited state wavefunction. This is a plausible result once the ground state $^3A_{2g}$ has a greater symmetry than the excited state $^3T_{2g}$ [28]. The greater symmetry of the ground state is much more sensible to an external perturbation than the excited state.

The negative values obtained for κ_2 (and β_{eff}), according to expression (5), indicate the *predominance* of an absorption saturation process occurring in the sample. If the process was due only to absorption saturation, then, by expression (5), $\beta_{eff} = \alpha/I_S$. Since this does not occur, as it is shown in Table 4, we must

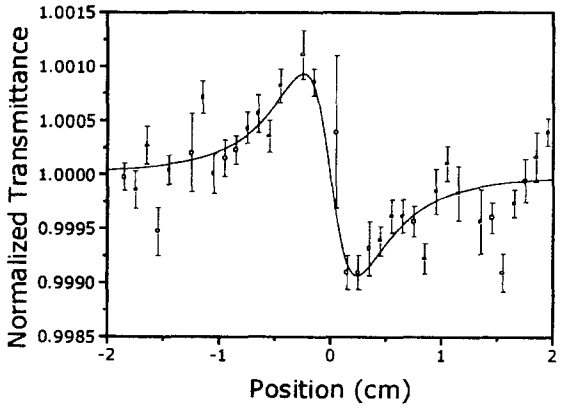

Fig. 4. Z-Scan curve for the sample with the smallest dopant concentration (0.15 mol.%). The intensity at the beamwaist position ($z = 0$) is $I = 14.1$ kW/cm^2. The peak–valley transmittance variation corresponds to a wavefront distortion of $\lambda/995$.

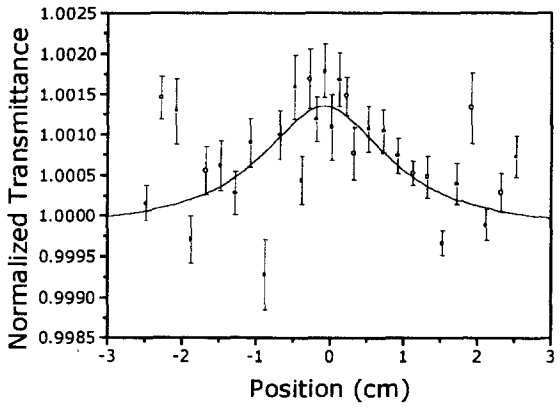

Fig. 5. Absorption curve for the sample with the greatest dopant concentration. The pumping beam intensity is 2.71 kW/cm^2 at the beamwaist position.

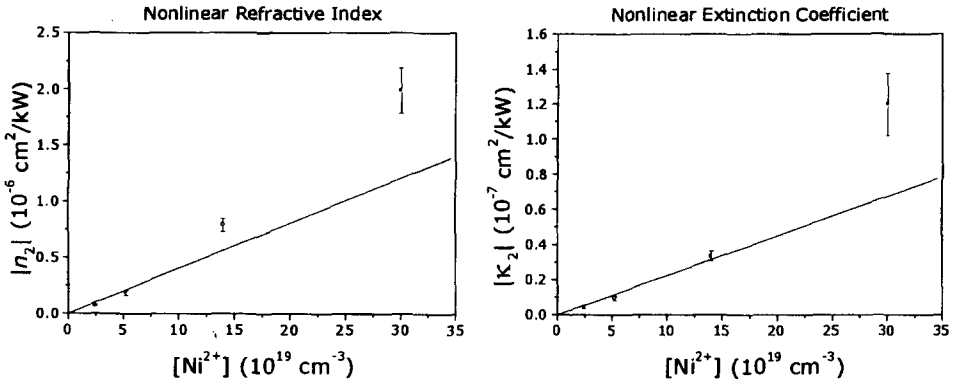

Fig. 6. In the left side graphic the concentration dependence of the modulus of n_2 for the samples are shown ($d|n_2|/d[Ni^2] = 2.24(29) \times 10^{-28}$); In the right side graphic the values are for the modulus of the nonlinear extinction coefficients ($d|\kappa_2|/d[Ni^{2+}] = 4.02(72) \times 10^{-27}$). In both cases the fit function goes through the origin.

Table 3. Values for the macroscopic and microscopic nonlinear parameters. The values of the nonlinear refractive indexes (n_2) and nonlinear extinction coefficients (κ_2) increase with the dopant concentration in the sample. The microscopic parameters γ_{eff} and β_{eff} are constant for low dopant concentration

Sample	$[Ni^{2+}]$ 10^{19} cm^{-3}	n_2 10^{-8} cm^2 kW^{-1}	γ_{eff} 10^{-27} cm^3	κ_2 10^{-9} cm^2 kW^{-1}	β_{eff}/ion 10^{-23} cm^{-2} kW^{-1}
0.15%	2.4(2)	−7.36(68)	−7.4(13)	−4.65(98)	−2.29(54)
0.30%	5.2(6)	−18.6(19)	−8.7(17)	−9.55(127)	−2.17(38)
1%	14(2)	−79.0(58)	−13.6(28)	−33.6(29)	−2.84(47)
2%	30(3)	−199(20)	−28.2(51)	−120(18)	−4.73(77)

conclude that there is an excited state absorption process occurring, weakening the saturation process. The expansion of expression (4) is incomplete, limited to a second order expansion, leading to an approximated expression for β_{eff} [expression (5)]. In order to obtain the excited state absorption cross-section, the expansion has to carry higher order terms. Within this limitations, it is only possible to obtain an approximation for the excited state absorption cross-section and the calculated value is constant to all samples and equal to $\sigma_3 = 3.36(13) \times 10^{-21}$ cm^2. We must reinforce that this value is an estimate in first-order and it corresponds to approximately the same value as the ground state absorption cross-section, shown in Table 2.

Table 4. Comparison between the values for the effective nonlinear absorption coefficient (β_{eff}) and the ratio α/I_S

Sample	α/I_S 10^{-3} cm kW^{-1}	β_{eff} 10^{-4} cm kW^{-1}
0.15%	3.62(55)	−5.5(14)
0.30%	8.1(11)	−11.3(24)
1%	21.0(33)	−39.8(87)
2%	32.1(66)	−142(27)

5. CONCLUSIONS

We measured the Ni^{2+} concentration dependence of the nonlinear coefficients of the $BaLiF_3 : Ni^{2+}$ crystal. With these samples we could develop a systematic study that allowed us to investigate the behavior of the nonlinearity as a function of the dopant concentration. We observed that the real and imaginary parts of the third order nonlinearity increase linearly with the concentration up to 1 mol.%. For higher concentrations the nonlinearity is higher than expected. These results corroborate the ones obtained by conventional spectroscopy, that indicate cooperative effects for Ni^{2+} concentration greater than 1 mol.%.

For the imaginary part, there is a competition between a saturation and an excited state absorption process and the negative value indicates that the saturation process dominates. We could estimate in first-order approximation, the value of the excited state absorption cross-section and have found it has a similar magnitude as the ground state absorption cross-section.

Acknowledgements—We would like to thank FAPESP, a state-founding agency, for supporting this work (FAPESP grants 93/4999-7 and 90/3712-8). One of us, R.E. Samad, also thanks to FAPESP for a scholarship (FAPESP 93/1367-0).

REFERENCES

1. Baldochi, S.L., Santo, A.M.E., Martins, E., Duarte, M., Vieira, M.M.F., Vieira, N.D. Jr. and Morato, S.P., *J. of Crystal Growth*, **166,** 1995, 375.
2. Moulton, P.F. and Mooradian, A., *Appl. Phys. Lett.*, **35,** 1979, 838.
3. Moncorgé, R. and Beyattou, T., *Phys. Rev.*, **B37,** 1988, 9186.
4. Martins, E., Vieira, N.D. Jr., Baldochi, S.L., Morato, S.P. and Gesland, J.Y., *J. of Luminescence*, **62,** 1994, 281.
5. Armstrong, J.A., Blombergen, N., Ducuing, J. and Pershan, P.S., *Phys. Rev.*, **127,** 1962, 1918.
6. Pershan, P.S., *Phys. Rev.*, **130,** 1963, 919.
7. Kelley, P.L., *Phys. Rev. Lett.*, **15,** 1965, 1005.
8. Chiao, R.Y., Garmire, E. and Townes, C.H., *Phys. Rev. Lett.*, **13,** 1964, 479.
9. Adair, R., Chase, L.L. and Payne, S.A., *Phys. Rev.*, **B39,** 1989, 3337.
10. Magni, V., Cerullo, G. and De Silvestri, S., *Opt. Commun.*, **96,** 1993, 348.
11. Sheik-Bahae, M., Said, A.A., Wei, T., Hagan, D.J. and Van Stryland, E.W., *IEEE J. of Quantum Elec.*, **QE-26,** 1990, 760.
12. Sheik-Bahae, M., Said, A.A. and Van Stryland, E.W., *Opt. Lett.*, **14,** 1989, 955.
13. Zhao, W. and Palffy-Muhoray, D., *Appl. Phys. Lett.*, **63,** 1993, 1613.
14. Xia, T., Hagan, D.J., Sheik-Bahae, M. and Van Stryland, E.W., *Opt. Lett.*, **19,** 1994, 317.
15. Ma, H. and de Araujo, C.B., *Appl. Phys. Lett.*, **66,** 1991, 1581.
16. Petrov, D.V., *J. Opt. Soc. Am.*, **B13,** 1996, 1491.
17. Yang, L., Dorsinville, R., Wang, Q.Z., Ye, P.X. and Alfano, R.R., *Opt. Lett.*, **17,** 1992, 323.
18. Wei, T.-H., Huang, T.-H. and Lin, H.-D., *Appl. Phys. Lett.*, **67,** 1995, 2266.
19. Pilla, V., Impinnisi, P.R. and Catunda, T., *Appl. Phys. Lett.*, **70,** 1997, 817.
20. Oliveira, L.C., Catunda, T. and Zilio, S.C., *Jpn. J. Appl. Phys.*, **35,** 1996, 2649.
21. Catunda, T. and Cury, L.A., *J. Opt. Soc. Am.*, **B7,** 1990, 1445.
22. Boling, N.L., Glass, A.J. and Owyoung, A., *IEEE J. of Quantum Elec.*, **QE-14,** 1978, 601.
23. Ashcroft, N.W. and Mermin, N.D., *Solid State Physics*, p. 557, W.B. Saunders Company, Philadelphia, 1976.
24. Jackson, R.A., Valério, M.E.G. and de Lima, J.F., *J. of Physics: Condensed Matter.*, **8,** 1996, 10931.
25. Chadwick, A.V., Davis, S.R., de Lima, J.F., Valério, M.E.G. and Baldochi, S.L., *J. of Physics: Condensed Matter.*, **8,** 1996, 10979.
26. Wetter, N.U., Maldonado, E.P. and Vieira, N.D. Jr., *Appl. Optics*, **32,** 1993, 5280.
27. Shen, Y.R., *The Principles of Nonlinear Optics*, p. 5. John Wiley & Sons Inc. New York, 1984.
28. Tanabe, Y. and Sugano, S., *J. of the Phys. Soc. of Japan*, **9,** 1954, 753.